

Application of Neutron Computed Tomography in Enhanced Oil Recovery for Analysing Oil Distribution in Berea Sandstone using Bagasse Surfactant

Rudarsko-geološko-naftni zbornik
(The Mining-Geology-Petroleum Engineering Bulletin)
UDC: 552.1
DOI: 10.17794/rgn.2023.5.8

Original scientific paper



Rini Setiati^{1*}; Fahrurrozi Akbar²; Gabriel Prasucipto Karisma³; Achmad Ramadhani⁴; Setiawan Setiawan⁵; Renato Aditya⁶; Muhammad Taufiq Fathaddin⁷; Sulistioso Giat Sukaryo⁸; Bharoto Bharoto⁹; Iwan Sumirat¹⁰

¹*Petroleum Engineering Department, Universitas Trisakti, Jalan Kiai Tapa, Jakarta, Indonesia, 11440, <https://orcid.org/0000-0001-9243-062X>*

²*National Research and Innovation Agency (BRIN) of the Republic of Indonesia, KST B. J. Habibie, Jalan Raya Puspiptek, Muncul, Kec. Setu, Kota Tangerang Selatan, Banten, Indonesia, 15310, <https://orcid.org/0000-0002-8838-1842>*

³*National Research and Innovation Agency (BRIN) of the Republic of Indonesia, KST B. J. Habibie, Jalan Raya Puspiptek, Muncul, Kec. Setu, Kota Tangerang Selatan, Banten, Indonesia, 15310, <https://orcid.org/0000-0002-2956-0963>*

⁴*National Research and Innovation Agency (BRIN) of the Republic of Indonesia, KST B. J. Habibie, Jalan Raya Puspiptek, Muncul, Kec. Setu, Kota Tangerang Selatan, Banten, Indonesia, 15310, <https://orcid.org/0000-0002-5437-8493>*

⁵*National Research and Innovation Agency (BRIN) of the Republic of Indonesia, KST B. J. Habibie, Jalan Raya Puspiptek, Muncul, Kec. Setu, Kota Tangerang Selatan, Banten, Indonesia, 15310, <https://orcid.org/0000-0002-7819-5843>*

⁶*Petroleum Engineering Department, Universitas Trisakti, Jalan Kiai Tapa, Jakarta, Indonesia, 11440, <https://orcid.org/0009-0007-4206-4896>*

⁷*Petroleum Engineering Department, Universitas Trisakti, Jalan Kiai Tapa, Jakarta, Indonesia, 11440, <https://orcid.org/0000-0003-2351-0292>*

⁸*National Research and Innovation Agency (BRIN) of the Republic of Indonesia, KST B. J. Habibie, Jalan Raya Puspiptek, Muncul, Kec. Setu, Kota Tangerang Selatan, Banten, Indonesia, 15310, <https://orcid.org/0009-0003-4830-3406>*

⁹*National Research and Innovation Agency (BRIN) of the Republic of Indonesia, KST B. J. Habibie, Jalan Raya Puspiptek, Muncul, Kec. Setu, Kota Tangerang Selatan, Banten, Indonesia, 15310, <https://orcid.org/0000-0003-0108-7673>*

¹⁰*National Research and Innovation Agency (BRIN) of the Republic of Indonesia, KST B. J. Habibie, Jalan Raya Puspiptek, Muncul, Kec. Setu, Kota Tangerang Selatan, Banten, Indonesia, 15310, <https://orcid.org/0000-0002-4764-1767>*

Abstract

The Neutron Computed Tomography (NCT) technique was adopted to study oil content within sandstone. In recent times, oil industries have turned to the Enhanced Oil Recovery (EOR) technique that uses chemicals/surfactants to reduce interfacial tension to maximize oil production from mature oil fields. The Berea core played a crucial role in investigating surfactant effectiveness for liberating trapped oil. The presented research is based on laboratory experiments carried out at the National Research and Innovation Agency and at the Trisakti University, Indonesia. The research proceeded in three steps. The first step was observation on the Berea core that is saturated with a low salinity brine of 40,000 ppm and 60,000 ppm and assessment of the total porosity of the sandstone. The second step included injecting oil into the sample and examining the water distribution. The final step was to inject sugarcane bagasse surfactant with 2% surfactant concentration to extract oil from the sandstone, then it was subjected to NCT analysis. The observations show that the pores are evenly distributed in the middle, the oil content accumulates at the edge, almost no oil remains in the middle of the Berea core after water injection, and the remaining oil returns to the main flow after surfactant injection. The results show that oil movement in the Berea core with 40,000 ppm salinity is better than oil movement with 60,000 ppm. The salinity of the brine can affect the mobility of oil droplets in the Berea core, and surfactant injection processes have better performance at lower salinity and are susceptible to higher salinity.

Keywords:

Neutron Computed Tomography; Enhanced Oil Recovery; bagasse surfactant; low salinity

1. Introduction

In recent decades, there is a noticeable decline in the initiation of new oil explorations. This decline has prompted increased interest in Enhanced Oil Recovery

(EOR), which represents a well-established technique for maximizing oil production from mature oil fields (Alvarado & Manrique, 2010; Bealesio et al., 2021; Massarweh & Abushaikha, 2020). EOR includes thermal, miscible, and chemical processes (Tapias Hernández & Moreno, 2020). This research focuses on the chemical technique using bagasse surfactant (Ali et al.,

Corresponding author: Rini Setiati

e-mail address: rinisetiati@trisakti.ac.id

2018), a by-product of sugar cane. Bagasse surfactant, used as an injection fluid at specific concentrations, is crucial in determining its efficacy within the Berea core medium. By reducing interfacial tension between oil droplets and rock surfaces, the surfactant enables oil droplets to move more freely toward production wells. The approach is supported by successful laboratory tests (Setiati, R. et al., 2018, 2019, 2020). Additionally, the combination of surfactant with low salinity injection has been reported to reduce capillarity and prevent excessive oil trapping (Johannessen & Spildo, 2013).

Several tools have been used to evaluate the EOR technique, including Fourier Transform Infra-Red (FTIR), Nuclear Magnetic Resonance (NMR) (Setiati et al., 2017; Wibowo, ADK., et al 2021; Nowrouzi, I., et al., 2022), Permeameter, and Pore-meter. These instruments represent common methods for assessing surfactant and reservoir rock quality (Esfandyari et al., 2021). Recent advancements introduce computed tomography (CT) as a complementary technique to the FTIR, NMR, Pore-meter and Permeameter. There are two types of CT methods, including X-ray CT (XCT) and neutron CT (NCT). High-resolution micro XCT, in particular, excels at indicating the liquid phase within the rock sample (Scheffer et al., 2021). CT also proves highly beneficial for understanding various processes such as pipe flow, separators, mixers, and reactors (Farrokhi et al., 2021; Johansen, G. A. 2013). Furthermore, the method is used to understand hydrocarbon in the reservoirs (Shiri, Y. et al., 2021; Mathisen et al., 1995), water quantification in fuel cells, and fluid flow in porous media (Fukahori et al., 2006; Heller, 2009; Shah et al., 2016).

NCT is a widely used method in the nuclear industry, particularly within science and engineering fields that investigate the internal structure and mechanical characteristics of materials. Over the years, NCT research has shown a growing trend, specifically since 2004, and the most promising one lies within EOR. The measurement method relies on neutrons sourced from nuclear reactors or synchrotrons, providing a distinct advantage for investigating elements with low atomic numbers, such as hydrogen and carbon (Schwarz et al., 2005; Penumadu & Kim, 2015; L'Annunziata, 2016). The earliest research incorporating the pore rock sample and neutron imaging was conducted by Frikkie De Beer and F. Middleton (De Beer & Middleton, 2006; De Beer et al., 2004). While their analysis did not specifically focus on reservoir rock samples, it piqued interest in applying NCT within the oil and gas industry. In late 2019, a collaboration between a nuclear analyst and an Indonesian university led to an in-depth investigation of Berea sandstone samples. The university team developed a new chemical formula from bagasse and explored the quantitative and qualitative effects of the surfactant in the EOR process (Pavan, 2022) through neutron imaging. Furthermore, the preliminary analysis addressed porosity measurement of Indonesian limestone (Akbar et al.,

2021) and visualization of the Berea sandstone sample (Setiati et al., 2021). The first step of porosity measurement research for the samples using NCT has also been published.

The research then progressed to investigate the permeability of the Berea sandstone sample, varying salinity at 40,000 ppm and 60,000 ppm with a 2.5% surfactant concentration. It aimed to visualize and non-destructively assess the oil content within the Berea sandstone of two samples. The research methodology incorporated immersing the samples in a brine water solution (Ansari et al., 2023) to analyze water distribution and measure porosities using NCT. The next step comprised injecting oil into the sandstone, releasing the oil trapped inside the sandstone sample with brine water flooding, and measuring the remaining oil content using NCT. Furthermore, the final phase introduced the bagasse surfactant to the sample and adopted NCT for measuring the trapped oil content. The result provided a 3D image of the oil within the sample and showed the distribution of oil content before and after surfactant flooding.

2. Materials and Methods

In the course of the experiments, two Berea sandstone samples, designated as C5 and C6, were subjected to investigation. The Berea core, a homogeneous synthetic core was used for assessing the effectiveness of surfactant in liberating trapped oil. The Berea core contains clean sandstone which has uniform porosity and permeability. The permeability is 500 mD and the porosity is 20.99%. Each core possessed a geometry of approximately 2.4cm in diameter and 4cm in height. The composition of the Berea core consists of 77.1% quartz (SiO_2), 5.3% kaolinite ($\text{Al}_2\text{Si}_2\text{O}_5(\text{OH})_4$), 2.6% montmorillonite, 2.5% albite, calcite, and 7.3% muscovite. In this study, synthetic Berea cores were used because of their homogeneity properties. This homogeneity is necessary to determine the characteristics of natural sugarcane bagasse surfactants. The natural performance of a

Table 1: Berea core components

Mineral	Berea (%w/w)
Quartz (SiO_2)	77.1
Kaolinite ($\text{Al}_2\text{Si}_2\text{O}_5(\text{OH})_4$)	5.3
Montmorillonite ($\text{CaO}_2(\text{AlMg})_2\text{Si}_4\text{O}_{10}(\text{OH})_2 \cdot 4\text{H}_2\text{O}$)	2.6
Calcite (CaCO_3)	-
Calcium silicate (CaSiO_3)	-
Albite, calcian, ordered ($\text{CaNa})\text{Al}(\text{SiAl})_3\text{O}_8$	2.5
$\text{NaO}_3(\text{AlMg})_2\text{Si}_4\text{O}_{10}(\text{OH})_2 \cdot 4\text{H}_2\text{O}$	-
Muscovite ($\text{KNa})\text{Al}_2(\text{SiAl})_4\text{O}_{10}(\text{OH})_2$	7.3
Hydrotalcite ($\text{Mg}_6\text{Al}_2\text{CO}_3(\text{OH})_{16} \cdot 4\text{H}_2\text{O}$)	-
Pumpellyite ($\text{Ca}_2\text{FeAl}_2(\text{SiO}_4)(\text{SiO}_7)(\text{OH})_2 \cdot \text{H}_2\text{O}$)	-

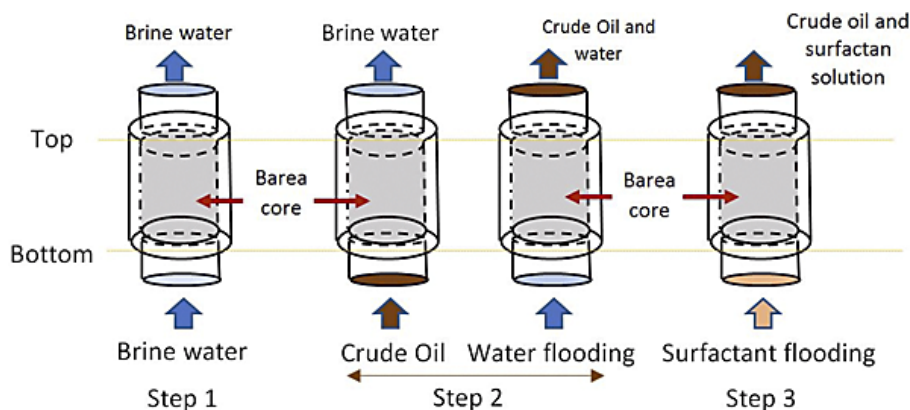


Figure 1: Three steps of the EOR application by using low salinity water and bagasse surfactant

surfactant is better tested in homogeneous rock conditions, such as the clean sandstone in the Berea core. **Table 1** below shows the components contained in the Berea core used in this research.

These two types of Berea cores were designated for injection with brines of varying salinity, specifically 40,000 ppm and 60,000 ppm, and a 2.5% surfactant concentration was consistently applied. The surfactant used in this research is sugarcane bagasse Sodium Lignosulfonate (SLS), which is synthesized from sugarcane bagasse. Several characteristics of the SLS bagasse surfactant that have been tested among others are that it is stable in aqueous mediums, capable of forming a middle phase emulsion of 6.25% in a mixture with light crude oil and has a static adsorption value of 8.07% and dynamic adsorption of 1.37%. The sugarcane bagasse SLS surfactant monomer has an HLB (Hydrophilic-Lipophilic Balance) value of 11.6, so it is categorized as an O/W (Oil in Water) emulsion, which indicates that the surfactant dissolves well in water.

Neutron Computed Tomography (NCT) is a 3-dimensional (3D) image from many 2-dimensional (2D) projections of samples taken at different angles. The NCT systems consist of three main parts: the neutron source, collimator, and detector. The BRIN's NCT facility uses a 15 MW nuclear research reactor with a neutron flux of 10^7 neutron/cm²s, the collimator guides the neutron into the research chamber with an L/D ratio of 87, and a 50 μ m Li₂ZnS scintillator screen. The NCT has a high-speed Andor's CMOS camera to record the data images, Octopus software to reconstruct the raw data into a tomographic image, and a Volume Graphic (VG) Studio Max for data analysis and 3D visualizations.

Before the NCT analysis, the stability of the bagasse surfactant, brine water salinity, and sandstone characteristics were rigorously tested.

The NCT investigations unfolded across three essential steps, as presented in **Figure 1**. In the first step, the Berea core was saturated with brine water. This comprised injecting brine water into the core until it reached a state of saturation. Both the two types of Berea cores

were saturated with brine, one at a concentration of 40,000 ppm and the other at 60,000 ppm. The brine saturation process typically spanned one to two days, marked by the absence of air bubbles. This statement is in accordance with previous research which stated the time used for the test (**Okon & Edoho, 2016**). These previous results can be used as a reference in conducting research. However, NCT measurements were executed to determine the porosities of the brine-saturated core before proceeding to subsequent stages.

The injection system was designed to ensure a bottom-to-top flow within the sample, minimizing the influence of gravitational effects. After saturating the sample with brine, it was carefully positioned within the NCT equipment to facilitate the observation and porosity measurement through tomography. It was crucial to observe that samples had to be wet before being subjected to NCT analysis. Additionally, NCT data acquisition was expedited after the sample was injected with brine water. The second step was the introduction of intermediate crude oil into the sandstone samples. Approximately 1ml to 1.2ml of crude oil was injected into the C5 and C6 samples, respectively. The volume of oil required for core saturation depended on the porosity and pore volume of the core. After the introduction of crude oil, the core was subjected to a 24-hour aging process to achieve complete saturation, which typically spanned two days. The second step also included oil extraction from the oil-saturated core through water injection, commonly referred to as waterflooding. In this process, the extracted oil was collected in a scaled pipette tube to quantify the volume of oil expelled during the water injection. The water injection process typically extended for approximately 1 to 1.5 pore volumes (PV) until no more oil was being discharged from the core. In the second step, there were two interconnected processes, including the injection of crude oil into the core to achieve saturation, followed by water injection, functioning as a drive mechanism for releasing the oil. This process comprised secondary recovery principles and upheld the concept of maintaining pressure within the core system. It was important to note that NCT imaging was not executed after

the crude oil injection but immediately after the water-flooding process. Once again, NCT data occurred promptly to prevent potential oil content evaporation and leakage.

The final step incorporated the injection of bagasse surfactant followed by the acquisition of NCT data. During this stage, surfactant was introduced into the Berea core, where it encountered the crude oil using specialized holder tools. The action of the surfactant within the core had a significant impact on altering the physical properties of crude oil, primarily by reducing interfacial tension, thereby facilitating the movement of oil droplets. The dispersion of surfactant within the Berea core was observable through NCT. Each sample was measured individually to prevent unwanted data interference, which could occur when samples were stacked or placed side by side.

NCT used neutrons generated by the G.A. Siwabessy Research Reactor, featuring a neutron flux of 10^7 n/cm²/second. Each image was exposed for 50 seconds, and a total of 360 image data sets were recorded. Tomographic images were reconstructed through Octopus software and optimized cross-section images using Fiji ImageJ software. The final image was reconstructed into a 3D model by stacking tomogram images with VG Studio Max. In the experiments, oil inside the sandstone appeared brighter, represented by a white colour, in contrast to the sandstone material. This research focused on presenting the results of the second and third steps, while the first step has been previously reported by Akbar et al. (2021) and R. Setiati et al. (2021). Porosity analysis and quantification of oil content within the sandstone were also performed. However, in the second and third steps, the experiments were specifically directed toward evaluating the remaining oil content inside the sandstone.

3. Results and Discussion

In the first step, NCT was adopted to investigate the distribution of porosity and its volume within the Berea core. The pores were consistently distributed across the central region of the core. It was important to note that a high porosity material does not always guarantee permeability.

There were layers within the Berea core sample (a), as confirmed by the tomographic image of NCT after one to two days of brine water injection (b). Another tomographic image was taken after the Berea core was soaked inside the brine water and found that the water was saturated (c).

Based on Figure 5, the second step (water flooding) indicated that oil content accumulated in the periphery (white colour) of the sandstone, with minimal oil remaining in the central region after water flooding.

The Berea core was injected with 100 mL - 120 mL of the intermediate oil (a). After the oil was saturated with-

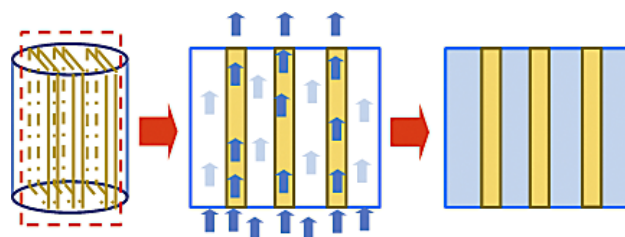


Figure 2: Illustration of step 1 of the process after brine injection

in the sandstone sample, the core was subjected to brine water flooding, resulting in 40% - 50% oil release, while the remaining 60% - 50% was pushed to the periphery of the core (b). The majority of the oil was retained in the periphery of the sandstone (c).

In the previous study (Setiati et al, 2019), it was known that most of the porosity (mostly a channel pores) was placed in the middle of the sandstone, so the most possible thing was that 40% - 50% of the oil was laid in the centre of the rock and swept out. This previous study is a research study that discusses water injection in a secondary recovery, without surfactants, where oil recovery can reach 40-50%. According to Al-Jifri (2021) and Zhao (2015), the advantages of produced water reinjections include increasing hydrocarbon production to around 45%-50.2%.

Based on Figure 4 and Figure 5, this contrasted with the results of the previous review in the second step, which showed that a significant portion of the porosity, mainly channel pores, was concentrated in the central region of the sandstone. However, after the injection of intermediate oil and water flushing, the oil did not flow from the central region of the Berea core. The cross-section image clearly showed that the oil was displaced to the periphery of the core. In Figure 3, the grey colour and the darker grey to black represented the sandstone material and pores, respectively. It was observed that several areas had large pores in the second step for C5 and C6, as indicated by the grey values falling within the pore/ void range. In the context of neutron interaction with matter, this image presented two possibilities, including whether it represented pores or another material transparent to neutrons. Neutrons interact with the nucleus of atoms, implying that their imaging does not depend on material density, unlike X-ray imaging (Lehmann, 2023; Alessandro et al., 2021; Peter, 2006). To definitively confirm the nature of these areas, XCT became the most powerful technique. XCT excelled at distinguishing between materials and pores, even though it could not detect materials with an atomic number (Z) lower than carbon (^{12}C). In the experiment, porosity could be largely disregarded because the primary focus was on the distribution of oil content before and after surfactant flooding.

Channel pores, connecting from the top to the bottom of the sample and positioned in the middle, facilitated

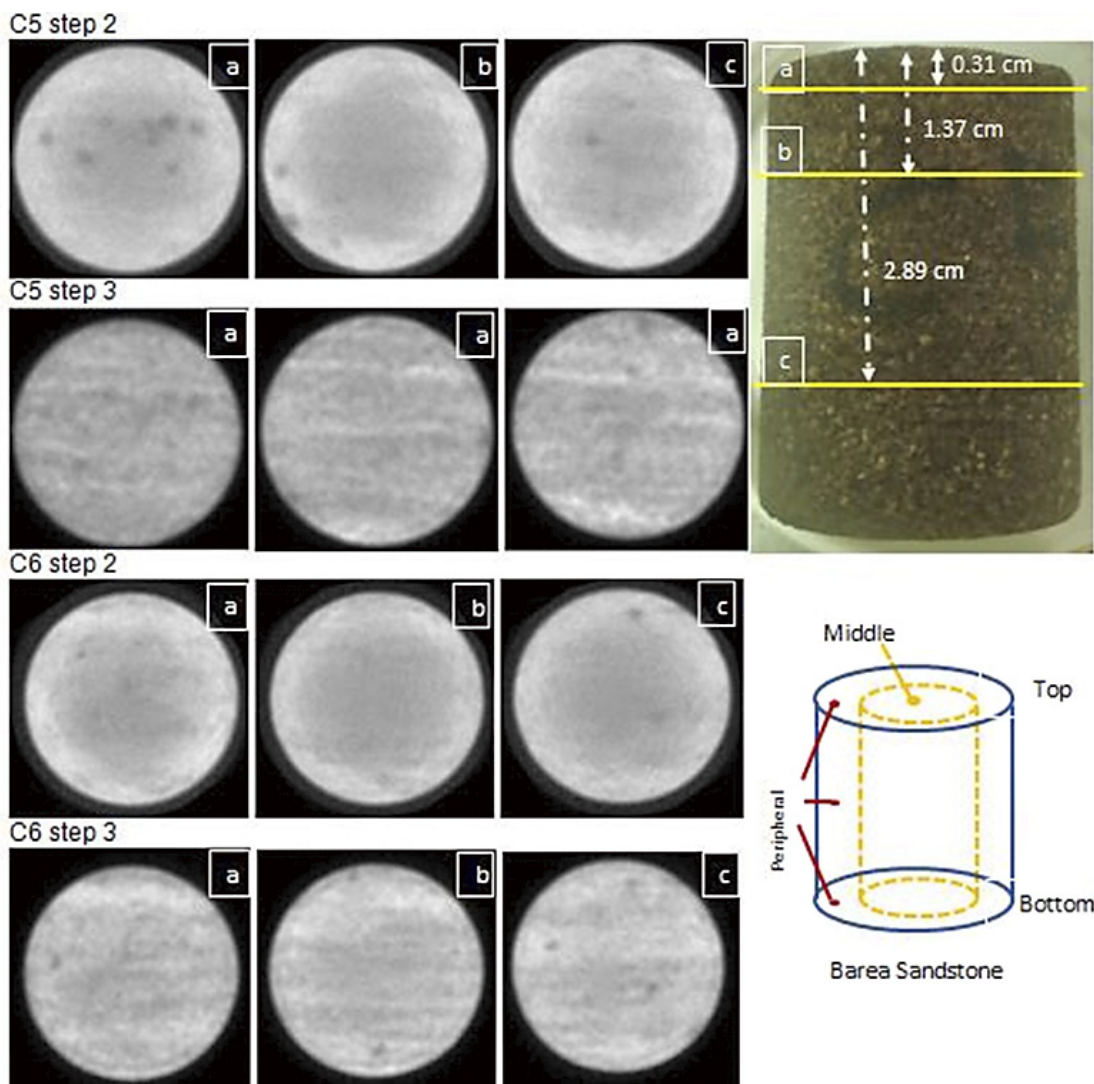


Figure 3: Three Cross-section images of C5 and C6

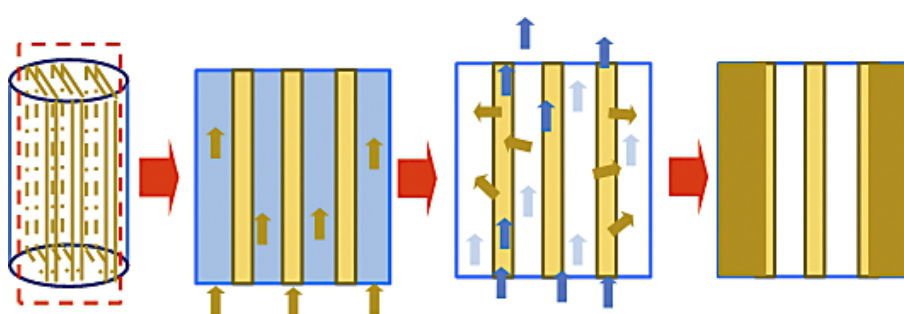


Figure 4: In step 2, after oil injection

the passage of (low) pressurized water from the bottom to penetrate the central area of the reservoir rock and displace the oil content inside the sandstone sample. Both samples were in pristine condition as they had not been subjected to treatment through primary (cracking with high-pressure gas) or secondary (high-pressure water) recovery applications.

Approximately three cross-section images of C5 and C6 from both the second and third steps respectively, are

shown in **Figure 3**. The cross-section images, denoted as 0.31 cm (a), 1.37 cm (b), and 2.89 cm (c), were measured from the top of the sandstone sample. The part of the sandstone area could be observed in the bottom right corner.

On the other hand, based on **Figure 6**, the third step of the experiment shows the residual oil migrating back towards the central flow path, particularly noticeable in **Figure 3** for C5 and C6. This reversal was attributed to

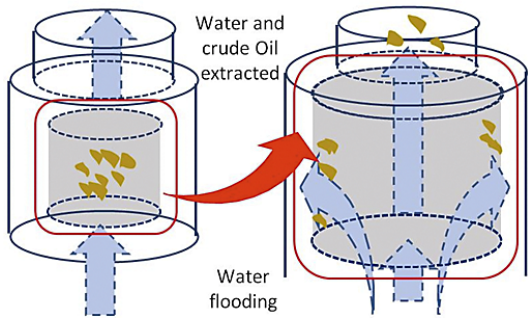


Figure 5: The water and oil content flow illustration after waterflooding processes

the reduction of interfacial tension (IFT) between crude oil and water due to the use of bagasse surfactant. The use of intermediate crude oil preceded the surfactant flooding, necessitating specific pre-processing. The third step for C5 and C6 showed not only the return of water to the primary flow path but also the formation of a white line pattern. The sandstone consisted of layers, which had differential permeability to oil after surfactant application, despite the decreasing IFT.

Figure 6 shows the results for the third step after the injection of bagasse surfactant (a). The bagasse surfactant effectively bound the oil and guided it to the permeable layers (b). Although several oil droplets were extracted, a portion remained within the Berea core sample. The oil droplets were not confined to the periphery of the sample but rather persisted within the permeable layers (c).

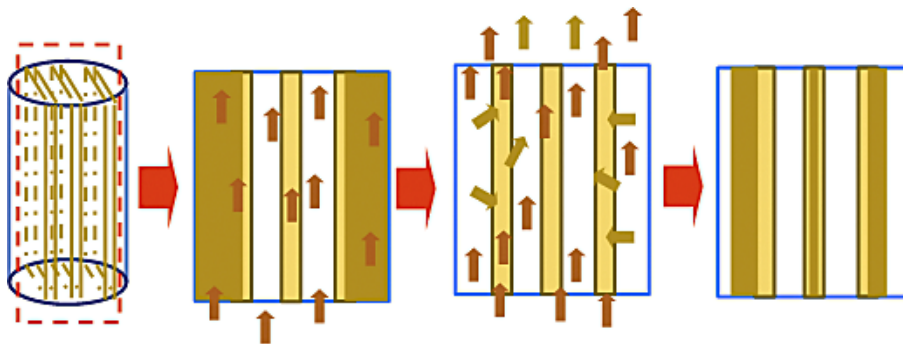


Figure 6: In step 3 after the bagasse surfactant injection

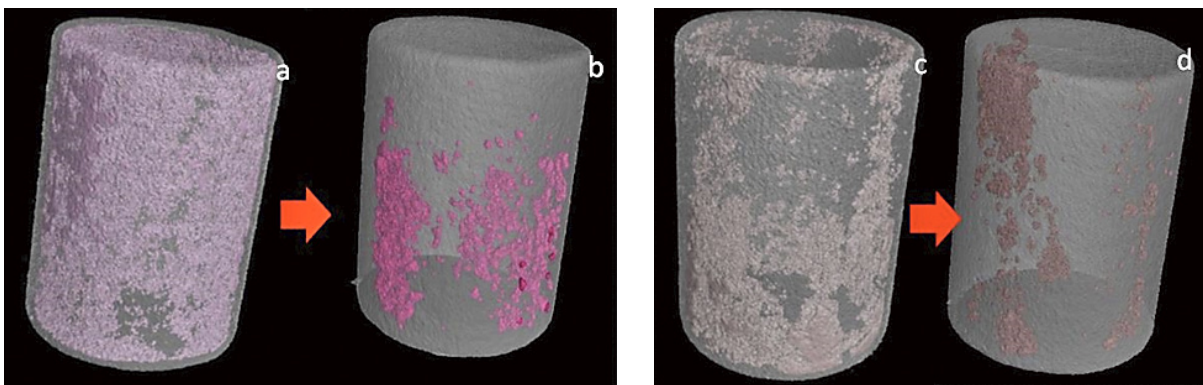


Figure 7: 3D visualization of oil content inside the C5 and C6 Berea sandstone samples

A visualization of C5 in the second step after water flooding with 40,000 ppm salinity (a) and after surfactant flooding with 60,000 ppm salinity (b) was presented. Additionally, visualization of C6 after water flooding (c) and after surfactant in the third step was provided. **Figure 7** showed that NCT effectively quantified the remaining crude oil content within the sandstone sample, with the necessity of conducting multiple repetitions to validate the observation. The experiment reaffirmed that the use of the lowest salinity water provided a significant advantage in extracting oil from the Berea core sample. This was validated through NCT measurements conducted after 14 days of the third step and subsequent storage of the samples in a specialized container with adjustable temperature and humidity. It was found that the C5 sample contained less crude oil than the C6, with an approximate oil escape rate of $\pm 84.65\%$ compared to $\pm 68\%$ for C5 and C6, respectively. The results were in line with the previous reviews that low salinity could reduce capillarity and mitigate oil entrapment within reservoir rocks. The reduction in capillarity facilitated enhanced oil mobility and subsequent extraction.

4. Conclusions

In conclusion, NCT successfully quantified the oil content within the sandstone sample, but for result reliability, multiple repetitions were advisable. The NCT technique generally substantiated the recommendation

for incorporating low salinity (LS) in Enhanced Oil Recovery (EOR) applications due to its positive impact on increasing oil extraction. At the culmination of the experimental processes, sample C5, treated with 40,000 ppm salinity, had a higher oil content escape rate compared to C6, which used 60,000 ppm salinity water, by approximately +/- 10%.

The 3D NCT imaging showed that during the second step of the experiment, the majority of the oil content congregated at the periphery. However, in the third step, crude oil tended to return to the central path (close to the centre of the rock sample). Previous reviews had identified the presence of a channel pore in the middle of the sandstone, which explained why during water flooding processes, approximately 40-50% of the oil flowed out from the channel pore. Consequently, the primary oil flow within the sandstone sample was situated in the middle.

Further exploration of NCT applications within the oil and gas industry, particularly in the context of EOR technology, is strongly suggested. Replicating experiments with limestone and sandstone are essential, but the availability of diverse samples could be a challenge. Collaboration with multiple industries was necessary to address these challenges. The next issue is maintaining brine water at 40,000 ppm and experimenting with various stable surfactant concentrations to assess their effectiveness within the sandstone sample. The introduction of Dynamic Neutron Imaging (DNI) could be a valuable addition to the experiment because it enabled real-time analysis of oil content flow paths and permeability changes before and after treatment. However, conducting DNI experiments would require advanced facilities, such as upgrading the Neutron Imaging facility by using multi-camera systems and transitioning from transmission to scattering methods.

Acknowledgement

The authors thank the Master of Petroleum Engineering at Universitas Trisakti and Research Centre for Radiation Detection and Nuclear Analysis Technology, for facilitating the funds and equipment for this research. The authors also extend their appreciation to the publisher for providing the opportunity for this article to be published.

5. References

- Akbar, F., Ramadhani, A., Gabriel, P. K., Bharoto, & Sulistiono, G. S. (2021): Porosity measurement and petrophysical properties of the Indonesian limestone as reservoir rock by using X-ray and neutron imaging technique. *AIPC*, 2381(1), 020003. <https://doi.org/10.1063/5.0066369>
- Al-Jifri M., Al-Attar H, Boukadi F, (2021): New proxy models for predicting oil recovery factor in waterflooded heterogeneous reservoirs, *Journal of Petroleum Exploration and Production* (2021) 11, 1443–1459, <https://doi.org/10.1007/s13202-021-01095-4>
- Ali, J. A., Kolo, K., Manshad, A. K., & Mohammadi, A. H. (2018): Recent advances in application of nanotechnology in chemical enhanced oil recovery: Effects of nanoparticles on wettability alteration, interfacial tension reduction, and flooding. In *Egyptian Journal of Petroleum* 27, (4). <https://doi.org/10.1016/j.ejpe.2018.09.006>
- Alvarado, V., & Manrique, E. (2010): Enhanced Oil Recovery: An Update Review. *Energies* 2010, Vol. 3, Pages 1529–1575, 3(9), 1529–1575. <https://doi.org/10.3390/EN3091529>
- Bealessio, B. A., Blázquez Alonso, N. A., Mendes, N. J., Sande, A. V. & Hascakir, B. (2021): A review of enhanced oil recovery (EOR) methods applied in Kazakhstan. *Petroleum*, 7(1), 1–9. <https://doi.org/10.1016/J.PETLM.2020.03.003>
- De Beer, F. C., & Middleton, M. F. (2006): Neutron radiography imaging, porosity and permeability in porous rocks. *South African Journal of Geology*. <https://doi.org/10.2113/gssajg.109.4.541>
- De Beer, F. C., Middleton, M. F., & Hilson, J. (2004): Neutron radiography of porous rocks and iron ore. *Applied Radiation and Isotopes*. <https://doi.org/10.1016/j.apradiso.2004.03.089>
- Esfandyari, H., Moghani, A., Esmaeilzadeh F., & Davarpanah, A. (2021): A Laboratory Approach to Measure Carbonate Rocks' Adsorption Density by Surfactant and Polymer. *Mathematical Problem in Engineering*. <https://www.hindawi.com/journals/mppe/2021/5539245/> <https://doi.org/10.1155/2021/5539245>
- Farrokhi, M., Jalalifar H., & Nasab S.M. (2021): An Evaluation of Cyclic Loading Conditions and Computed Tomography for the Strength and Petrophysical Properties of Anhydrite Caprock. (*The Mining-Geology-Petroleum Engineering Bulletin*). *Rudarsko-geološko-naftni zbornik*, 36 (4) DOI: 10.17794/rgn.2021.4.11
- Fukahori, D., Saito, Y., Morinaga, D., Ogata, M., Sugawara, K. (2006): Study on Water Flow in Rock by Means of the Tracer-aided X-rays CT in: Desrués, J., Viggiani, G., Bésuelle, P (eds): *Advances in X-ray Tomography for Geomaterials* - John Wiley & Sons, Inc. <https://doi.org/10.1002/9780470612187.ch28>
- Heller, A.K., Shi, L., Brenizer, J.S., Mench, M.M. (2009): Initial water quantification results using neutron computed tomography, *Nuclear Instruments and Methods in Physics Research Section A: Accelerators, Spectrometers, Detectors and Associated Equipment*, 605, (1–2), 99–102, ISSN 0168-9002, <https://doi.org/10.1016/j.nima.2009.01.166>.
- Hernández, T. F. A., & Moreno, R. B. Z. L. (2020): The effectiveness of computed tomography for the experimental assessment of surfactant-polymer flooding. *Oil & Gas Science and Technology – Revue d'IFP Energies Nouvelles*, 75, 5. <https://doi.org/10.2516/OGST/2019069>
- Johannessen, A. M., & Spildo, K. (2013): Enhanced oil recovery (EOR) by combining surfactant with low salinity injection. *Energy and Fuels*, 27(10), 5738–5749. <https://doi.org/10.1021/EF400596B>
- Johansen, G. A. (2013): *Emerging Tomographic Methods within the Petroleum Industry*. 2013 International Nuclear Atlantic Conference – INAC, 24–29. ISBN: 978-85-99141-05-2.

- L'Annunziata, M. F. (2016): Chapter 1 - Radioactivity and Our Well-Being, Editor(s): Michael F. L'Annunziata, Radioactivity (Second Edition), Elsevier, 1-66, ISBN 9780444634894, <https://doi.org/10.1016/B978-0-444-63489-4.00001-0>.
- Lehmann, H.E. (2023): Basics of Neutron Imaging. IntechOpen. doi: 10.5772/intechopen.110403
- Massarweh, O., & Abushaikha, A. S. (2020): The use of surfactants in enhanced oil recovery: A review of recent advances. *Energy Reports*, 6, 3150–3178. <https://doi.org/10.1016/j.egy.2020.11.009>
- Mathisen, M. E., Vasiliou, A. A., Cunningham, P., Shaw, J., Justice, J. H., & Guinzy, N. J. (1995): Time-lapse cross-well seismic tomogram interpretation: implications for heavy oil reservoir characterization, thermal recovery process monitoring, and tomographic imaging technology. *Geophysics*, 60(3). <https://doi.org/10.1190/1.1443803>
- Nowrouzi I., Mohammadi, AH., Manshad, AK. (2022): Preliminary Evaluation of A Natural Surfactant Extracted from Myrtus Communis Plant for Enhancing Oil Recovery from Carbonate Oil Reservoirs, *Journal of Petroleum Exploration and Production Technology*, 12, 783-792.
- Okon, A., & Edoho, U. (2016): Experimental Study of Brine Concentration Effect on Reservoir Porosity and Permeability Measurement. *Journal of Scientific Research and Reports*, 12(2). <https://doi.org/10.9734/jsrr/2016/28930>
- Pavan, N. V. T., Devarapu, S.R. & Govindarajan, S.K. (2022): Comparative Analysis On Impact Of Water Saturation On The Performance Of In-Situ Combustion. *Rudarsko-geološko-naftni zbornik*, 37 (4), 167-175. <https://doi.org/10.17794/rgn.2022.4.14>
- Penumadu, D., Kim, F.H. (2015): Chapter 8 - Multimodal Radiation Based Tomography and Diffraction of Granular Materials Using Neutrons and Photons and Instrumented Penetration Mechanics, Editor(s): Magued Iskander, Stephan Bless, Mehdi Omidvar, Rapid Penetration into Granular Media, Elsevier, 2015, Pages 267-290, ISBN 9780128008683, <https://doi.org/10.1016/B978-0-12-800868-3.00008-0>.
- Schwarz, D., Vontobel, P., Lehmann, E.H., Meyer, C.A., & Bongartz, G. (2005): Neutron Tomography Of Internal Structures Of Vertebrate Remains : A Comparison With X-Ray Computed Tomography.
- Scheffer, K., Méheust, Y., Carvalho, M. S., Mauricio, M. H. P., & Paciornik, S. (2021): Enhancement of oil recovery by emulsion injection: A pore scale analysis from X-ray micro-tomography measurements. *Journal of Petroleum Science and Engineering*, 198, 108134. <https://doi.org/10.1016/J.PETROL.2020.108134>
- Setiati, R., Siregar S., Marhaendrajana. T., Wahyuningrum D, (2017): Infra Red Evaluation of Sulfonation Surfactant Sodium Lignosulfonate on Bagasse: The International Journal of Science and Technoledge, (ISSN 2321 – 919X) Vol 5 Issue 3, March 2017 pp 137 – 142. www.theijst.com
- Setiati, R., Siregar, S., Marhaendrajana, T., & Wahyuningrum, D. (2018): Influence of middle phase emulsion and surfactant concentration to oil recovery using SLS surfactant synthesized from bagasse. *IOP Conference Series: Earth and Environmental Science*, 212(1). <https://doi.org/10.1088/1755-1315/212/1/012076>
- Setiati, R., Sumirat, I., Sukaryo, S. G., Adisoemarta, P. S., Akbar, F., Marpaung, T., Bharoto, B. (2021): Visualizations of Berea sandstone pores using neutron tomography. *E&ES*, 894(1), 012010. <https://doi.org/10.1088/1755-1315/894/1/012010>
- Setiati, R., Siregar, S., Marhaendrajana, T., & Wahyuningrum, D. (2019): Surfactant Flooding for EOR Using Sodium Lignosulfonate Synthesized from Bagasse. *Enhanced Oil Recovery Processes - New Technologies*. <https://doi.org/10.5772/INTECHOPEN.88689>
- Setiati, R., Siregar, S., Marhaendrajana, T., & Wahyuningrum, D. (2020): Enhanced oil recovery using synthesized sodium lignosulfonate surfactant from bagasse as development petroleum science. *AIP Conference Proceedings*, 2245(1), 090015. <https://doi.org/10.1063/5.0007725>
- Shah, S.M., Gray, F., Crawshaw, J.P., Boek, E.S. (2016): Micro-computed tomography pore-scale study of flow in porous media: Effect of voxel resolution, *Advances in Water Resources*, Volume 95, 2016, Pages 276-287, ISSN 0309-1708, <https://doi.org/10.1016/j.advwatres.2015.07.012>.
- Shiri, Y. & Shiri, A. (2021): Numerical Investigation of Fluid Flow Instabilities in Pore-Scale with Heterogeneities in Permeability And Wettability. *Rudarsko-geološko-naftni zbornik*, 36 (3), 143-156. <https://doi.org/10.17794/rgn.2021.3.10>
- Wibowo, ADK., Tiani, P., Aditya, L., Handayani, AS., and Christwardana, M., (2021): Synthesis and Characterization of Polymeric Surfactant from Palm Oil Methyl Ester and Vinyl Acetate for Chemical Flooding, *Reaktor*, 21 (2), 65-73 <https://ejournal.undip.ac.id/index.php/reaktor/>
- Zhao, L., Chen, X., Chen, L. Cao, R., Zhang, X., Liu, J., Shan, F. (2015): Effects of oil recovery rate on water-flooding of homogeneous reservoirs of different oil viscosity, *Petroleum Exploration and Development*, 42, (3), 384-389. ISSN 1876-3804, [https://doi.org/10.1016/S1876-3804\(15\)30029-X](https://doi.org/10.1016/S1876-3804(15)30029-X).

SAŽETAK

Primjena neutronske tomografije u kemijskoj metodi povećanja iscrpka nafte upotrebom bagasa kao surfaktanta za analizu distribucije nafte u pješčenjaku Berea

Za utvrđivanje sadržaja nafte u pješčenjaku primijenjena je neutronska kompjuterizirana tomografija (engl. *Neutron Computed Tomography*, NCT). U posljednje se vrijeme u naftnoj industriji sve više primjenjuje tehnika povećanja iscrpka nafte (engl. *Enhanced Oil Recovery*, EOR) koja upotrebljava kemikalije/surfaktante za smanjenje međupovršinske napetosti kako bi se povećala proizvodnja nafte iz starih naftnih polja. Jezgra pješčenjaka Berea odigrala je ključnu ulogu u istraživanju učinkovitosti surfaktanta za oslobađanje zarobljene nafte. Predstavljeno istraživanje temelji se na laboratorijskim istraživanjima provedenim u Nacionalnoj agenciji za istraživanje i inovacije i na Sveučilištu Trisakti iz Indonezije. Istraživanje je provedeno u tri koraka. U prvome koraku utvrđena je ukupna poroznost pješčenjaka temeljem istraživanja provedenih na jezgri pješčenjaka Berea, koja je zasićena slanom vodom niskoga saliniteta 40 000 ppm te vodom saliniteta 60 000 ppm. U drugome koraku u jezgri je utiskana nafta te se pratila distribucija vode. U posljednjemu koraku u jezgri je, kao surfaktant, utiskana bagasa u koncentraciji od 2 % kako bi se iz jezgre izdvojila nafta, a zatim je jezgra podvrgnuta neutronske kompjuteriziranoj tomografiji. Analizom rezultata NCT-a utvrđena je ravnomjerna distribucija pora u sredini jezgre, nakupljanje nafte u rubnim dijelovima, pri čemu, nakon utiskivanja vode, u središnjemu dijelu nema nafte, a preostala se nafta pokreće nakon utiskivanja surfaktanta. Rezultati pokazuju da je kretanje nafte u jezgri pješčenjaka Berea zasićenoj vodom saliniteta 40 000 ppm bolje nego u onoj zasićenoj vodom saliniteta 60 000 ppm. Salinitet slane vode može utjecati na pokretljivost kapljica nafte u jezgri pješčenjaka Berea, a surfaktant ima veću učinkovitost pri nižemu salinitetu te je osjetljiv na viši salinitet.

Ključne riječi:

neutronska kompjuterizirana tomografija, metoda povećanja iscrpka nafte, surfaktant bagasa, niski salinitet

Author's contribution

Rini Setiati (1) (Dr, Petroleum Engineering, lecturer, expertise in Enhanced Oil Recovery) has proven the mechanism of action of surfactant flooding on EOR. **Fahrurrozi Akbar (2)** (M.Sc., Researcher/ Instrument Scientist) performed neutron tomography data analysis, measurement and interpretation results. **Gabriel Prasucipto Karisma (3)** (Diploma III Nuclear Administration Research Mechanic) took the tomography images data at RSG GA Siwabessy. **Achmad Ramadhani (4)** (B.Eng., Nuclear Technology Developer/ Electric and Mechanic) took the tomography images data at RSG GA Siwabessy. **Setiawan Setiawan (5)** (Technician/ Mechanic) prepared the neutron radiography chamber and made sure the tomography system worked well. **Renato Aditya (6)** (M.Eng., Petroleum Engineering) prepared cores for analysis by neutron tomography. **Muhammad Taufiq Fathaddin (7)** (Ph.D., Associate Professor, Petroleum Engineering) analyzed the results of the neutron tomography interpretation of the performance of the oil mechanism. **Sulistio-so Giat Sukaryo (8)** (M.Sc., Researcher/ Material Scientist) contributed to the manuscript editing and interpretation of the results. **Bharoto Bharoto (9)** (M.Sc., Researcher/ Computer Scientist) prepared the data acquisition of neutron tomography software. **Iwan Sumirat (10)** (Dr. Eng., Researcher/ Instrument Scientist at Neutron Scattering) set up the neutron tomography experiment method.